JDR
JOURNAL OF DENTAL RESEARCH®
Featuring Critical Reviews in Oral Biology & Medicine

VOLUME 84 • NUMBER 8 • AUGUST 2005

Fusobacterium nucleatum Apoptosis-inducing Outer Membrane Protein

C.W. Kaplan, R. Lux, T. Huynh, A. Jewett,
W. Shi, and S. Kinder Haake

The FREE AND FINAL version of this paper & its added data and links are on the journal Web site.

RAPID COMMUNICATION
Biological

C.W. Kaplan[1], R. Lux[3], T. Huynh[3], A. Jewett[3], W. Shi[1,2,3], and S. Kinder Haake[3]*

[1]Molecular Biology Institute, [2]Department of Microbiology, Immunology and Molecular Genetics, and [3]Department of Oral Biology and Oral Medicine, Dental Research Institute, Section of Periodontics, UCLA School of Dentistry, 10833 Le Conte Ave., Los Angeles, CA 90095-1668; *corresponding author, shaake@dent.ucla.edu

J Dent Res 84(8):700-704, 2005

Fusobacterium nucleatum Apoptosis-inducing Outer Membrane Protein

ABSTRACT

The periodontal pathogen *Fusobacterium nucleatum* induces apoptosis in lymphocytes. We previously identified the autotransporter protein Fap2 in *F. nucleatum* strain PK1594 that induced apoptosis in lymphocytes when expressed in *Escherichia coli*. In this study, we identified protein homologs of Fap2 in the transformable *F. nucleatum* strain ATCC 23726, to determine their role in the induction of apoptosis in lymphocytes. We used a new gene-inactivation vector conferring thiamphenicol resistance (pHS31) to construct a mutant deficient in one of the homologs, *aim*1. Transcriptional analyses demonstrated disruption of *aim*1 expression, and phenotypic analyses revealed a 41% decrease in the ability of the mutant to induce apoptosis in Jurkat cells, as compared with the parental strain. These studies demonstrate, in the native host cell background, the contribution of *aim*1 to *F. nucleatum* induction of apoptosis and, to the best of our knowledge, represent the first report of a genetically defined and phenotypically characterized mutation in *F. nucleatum*.

KEY WORDS: *Fusobacterium nucleatum*, apoptosis, autotransporter, *aim*1, mutant.

Received February 28, 2005; Last revision May 31, 2004; Accepted June 1, 2005

INTRODUCTION

Fusobacterium nucleatum is a Gram-negative, anaerobic fusiform bacterium implicated as one of the causative agents of periodontal disease (Bolstad *et al.*, 1996; Moore *et al.*, 1982a,b, 1984, 1985), a chronic polymicrobial infection affecting the supporting tissues of teeth. Bacteria present in dental plaque advance the disease process by irritating tissues, leading to bone and attachment loss. The pathogenesis of *F. nucleatum* is not limited to the oral cavity; it is associated with a variety of systemic conditions, giving its pathogenesis broader relevance to the medical community (Sabiston and Gold, 1974; Sundqvist *et al.*, 1979; Ribot *et al.*, 1981; Edson *et al.*, 1982; Truant *et al.*, 1983; Gonzalez-Gay *et al.*, 1993; Jousimies-Somer *et al.*, 1993; Talan *et al.*, 1999; Heckmann *et al.*, 2003). *F. nucleatum* pathogenesis is still poorly understood, but the development of a genetic system (Haake *et al.*, 2000) and sequencing of 3 strains (Kapatral *et al.*, 2002, 2003) now enables the underlying mechanisms to be investigated at a molecular level.

Our previous research shows that *F. nucleatum* induces apoptosis in lymphocytes, an ability mediated by heat-labile outer membrane protein(s) that may allow the micro-organism to evade the immune system (Jewett *et al.*, 2000). To identify the protein(s) involved, we expressed an *F. nucleatum* PK1594 gene library in *E. coli* and subjected the clones to cell death assays with lymphocytes. Five genes that mediated increased apoptosis in lymphocytes were found (unpublished observations). One of these genes, Fap2, showed homology to an autotransporter protein family. This was particularly interesting, since similar proteins have been identified as virulence factors in other bacteria (Henderson and Nataro, 2001).

In this study, we sought to establish the role of Fap2 in inducing apoptosis in lymphocytes. A genetic system to transform *F. nucleatum* was available, but strain PK1594 remained refractory to genetic manipulation. An integration vector (pHS31) possessing a *cat*P gene capable of conferring thiamphenicol resistance in *F. nucleatum* was constructed. We used pHS31 to create a mutation in a Fap2 homolog in the transformable *F. nucleatum* strain ATCC 23726, and designated it *aim*1 (apoptosis inducing membrane protein gene 1), since transcriptional and phenotypic analyses demonstrated a role for this gene in inducing apoptosis in Jurkat cells. These data constitute, to the best of our knowledge, the first report of a genetically defined and phenotypically characterized mutation in *F. nucleatum*, and a genetic basis for its ability to induce apoptosis in lymphocytes.

MATERIALS & METHODS

Bacterial Strains, Cell Lines, and Culture Conditions

F. nucleatum strains were cultivated on Columbia agar or in Columbia broth (Difco, Detroit, MI, USA). Thiamphenicol (MP Biomedicals, Irvine, CA, USA) at 5 μg/mL was used for selection and maintenance of strains possessing the *cat*P determinant. Jurkat cells were maintained in RPMI 1640 supplemented

with 1 mM sodium pyruvate, 0.1 mM non-essential amino acids, 10 U/mL penicillin, 10 mg/mL streptomycin (Life Technologies, Grand Island, NY, USA), and 10% fetal calf serum (Irvine Scientific, Santa Ana, CA, USA).

Protein Analyses and Construction of a *Fusobacterium nucleatum* Mutant

Protein sequence homology was determined by use of the BLAST 2 program on the NCBI Web site (Tatusova and Madden, 1999). *Aim*1 mutants were created by single homologous recombination with the integration plasmid pHS31. Plasmid pHS31 was constructed from pJIR750, a clostridial shuttle plasmid possessing the *cat*P gene conferring thiamphenicol resistance in *F. nucleatum*. Plasmid pJIR750 was digested with *Xba*I and *Spe*I, followed by isolation of the DNA fragment possessing the ColE1 origin and *cat*P gene, and re-ligated to generate pHS31. The *aim*1 gene fragment, designated *aim*1′, was amplified with *Taq* DNA polymerase with use of the primers *aim*1F′ and *aim*1R′(Table 1), and cloned into the vector pCR2.1 (Invitrogen, Carlsbad, CA, USA). The fragment was excised from the pCR2.1 vector by *Eco*RI, blunted, gel-purified, and ligated into a blunt-ended, dephosphorylated pHS31 to generate pIP-*aim*1. *E. coli* was transformed with the ligation reaction, and the resulting integration plasmid was confirmed by restriction analysis and PCR. *F. nucleatum* transformation was performed as previously described (Haake *et al.*, 2000).

Transcriptional Analyses

Genomic DNA was extracted from stationary-phase cells following standard protocols.

Total RNA was extracted from mid-log-phase cells according to a hot-phenol protocol (Merritt *et al.*, 2005). A 3-μg quantity of total RNA was used for cDNA synthesis by Stratascript RT (Stratagene, La Jolla, CA, USA), according to the manufacturer's protocol. For real-time RT-PCR, SYBR green (Bio-Rad, Hercules, CA, USA) was used for fluorescence detection with the iCycler real-time PCR system (Bio-Rad), according to the manufacturer's protocol. Statistical analysis was performed by analysis of variance (ANOVA) with SPLUS 6.0 (Insightful, Seattle, WA, USA).

DNA Staining and Apoptosis Assay

We assessed apoptosis, based on DNA staining, by labeling the cells with propidium iodide as described previously (Jewett *et al.*, 2000). Briefly, samples of 2 x 10^5 cells were washed twice with PBS and incubated in 70% ethanol on ice. After 30 min of incubation, the cells were washed twice with PBS and 70 μL of RNase (1 mg/mL; Sigma), and a 140-μL quantity of propidium iodide (100 mg/mL; Sigma) was added to each sample. After incubation for 1 hr, analysis was performed with the use of a flow cytometer (Beckman Coulter, Fullerton, CA, USA). Each assay was run in 3 independent experiments to confirm reproducibility. Statistical analysis was performed as stated above.

Table 1. Primers Used in This Study

Primer	Sequence
catP-F	5′-TTAGGACGGCAATCAATCAA-3′
catP-R	5′-AAACGGCAAATGTGAAATCC-3′
ColE1	5′-GCAGAGCGAGGTATGTAGGC-3′
*aim*1′F	5′-CTGTTGGGAAAGAAGGAGTTG-3′
*aim*1′R	5′-TTGAATAAAGGGCTGCTGTG-3′
*aim*1-5′F	5′-GTTTGGAGCAGGAGGTTCAA-3′
*aim*1-3′R	5′-CCTTGGCATCATTTTCAATAGTT-3′
2057rt-F	5′-AAAAGAAGCCGATAAAAATGG-3′
2057rt-R	5′-ATCACTGGGTATTGTCCTTGTTC-3′
DSrt-F	5′-CCATCTGCGTCCGTTATTGT-3′
DSrt-R	5′-GGAACTGCTGGTGGAGATAAG-3′
DS2rt-F	5′-TTGTCCTGGATCAGTAACAGAAAG-3′
DS2rt-R	5′-CCTAAAGGTGGAAGAACGAAGA-3′
USrt-F	5′-CCTGCTCCAAACATTCCAAC-3′
USrt-R	5′-AGTGAAACAACAACAGCAATGG-3′
Control rt-F	5′-GGTTAAGTCCCGCAACGA-3′
Control rt-R	5′-CATCCCCACCTTCCTCCTAC-3′

RESULTS

Identification of Fap2 Homologs in *F. nucleatum* ATCC 23726

We previously identified the apoptosis-inducing autotransporter protein, Fap2, in *F. nucleatum* PK1594, based on its ability to induce apoptosis in lymphocytes when expressed in *E. coli* (unpublished observations). Because PK1594 is not amenable to genetic manipulation, Fap2 homologs were identified in the transformable *F. nucleatum* strain ATCC 23726. Since the *F. nucleatum* ATCC 23726 genome has not been sequenced, thus precluding direct analysis, homologs were first identified in the sequenced strain ATCC 25586, which is related to ATCC 23726 at the subspecies level. We used a local BLAST search and identified 8 predicted outer-membrane proteins with homology to Fap2 (Table 2). We then confirmed that the Fap2 homologs encoded by the ATCC 25586 genome were equally present in ATCC 23726 by partially sequencing each of the

Table 2. Predicted Outer Membrane Protein Homology to Fap2 and *F. nucleatum* ATCC 23726 Homologs

ATCC 25586 Fap2 Homologs	Genome Annotation	Predicted Protein Length (aa)	PK1594 Fap2 (3692 aa) Identities	PK1594 Fap2 (3692 aa) Positives	ATCC 23726 Sequenced Fragment Identities	ATCC 23726 Sequenced Fragment Positives
Fn0254	outer membrane protein	1677	675/1852 (36%)	930/1852 (49%)	322/322 (100%)	322/322 (100%)
Fn0387	probable outer membrane protein	1724	615/1879 (32%)	900/1879 (47%)	251/251 (100%)	251/251 (100%)
Fn1449	outer membrane protein	3165	2025/3347 (60%)	2407/3347 (71%)	442/453 (97%)	446/453 (97%)
Fn1526	predicted outer membrane protein	2143	597/2411 (24%)	981/2411 (39%)	317/322 (98%)	319/322 (98%)
Fn1554	predicted outer membrane protein	1582	652/1815 (35%)	909/1815 (49%)	292/292 (100%)	292/292 (100%)
Fn1893	predicted outer membrane protein	1361	546/1418 (38%)	760/1418 (53%)	287/287 (100%)	287/287 (100%)
Fn2047	predicted outer membrane protein	1630	638/1736 (36%)	890/1736 (50%)	264/270 (97%)	266/270 (97%)
Fn2058 (aim 1)	predicted outer membrane protein	1794	677/1975 (34%)	970/1975 (48%)	1765/1791 (98%)	1772/1791 (98%)

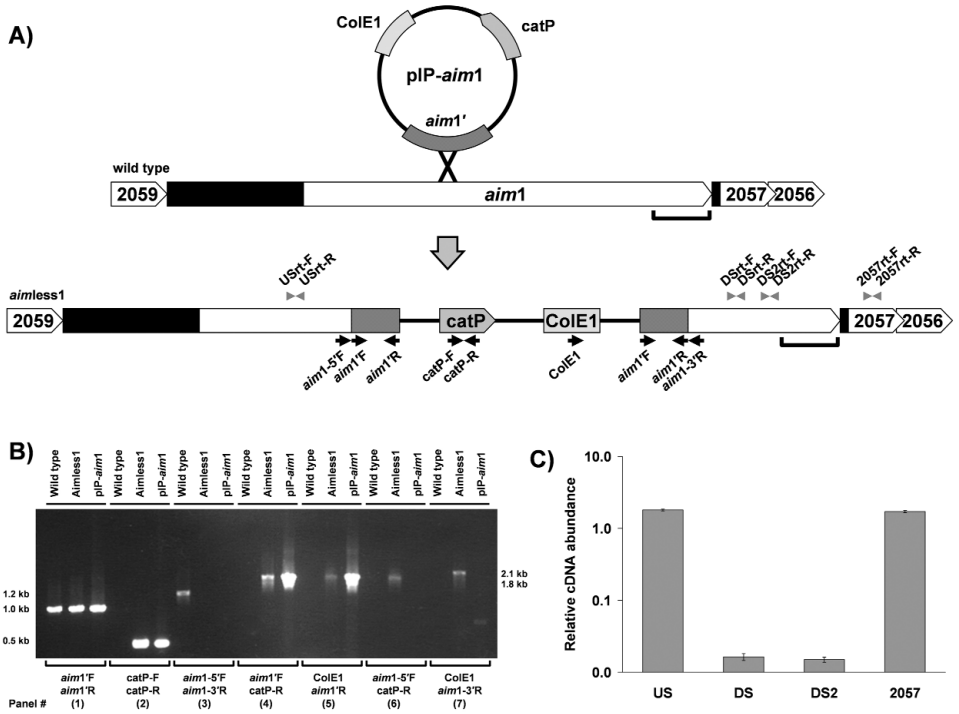

Figure 1. Structural and transcriptional analyses of wild-type and *aim*less1 mutant strains. **(A)** Schematic illustration of mutagenesis: organization of *aim*1 and flanking genes on the *F. nucleatum* ATCC 23726 wild-type and *aim*less1 mutant chromosome. Arrows indicate PCR primers used for construction and analysis of the *aim*1 mutant; arrowheads indicate real-time PCR primers; black shaded area indicates intergenic region; bracket indicates location of autotransporter domain. Full-length *aim*1 (5625 bases) was submitted to GenBank and has been assigned accession number DQ020251. The Fig. is not to scale. **(B)** PCR analysis confirming insertion into *aim*1. PCR analysis of chromosomal DNA from ATCC 23726 and the *aim*less1 mutant. Plasmid pIP-*aim*1, the construct used to create the inactivation in *aim*1, was used as the control DNA template. **(C)** Transcriptional analysis of *aim*1 and the downstream gene Fn2057. The relative RNA abundance of *F. nucleatum* wild-type and *aim*less1 was determined by real-time PCR. Results are expressed as relative means (mutant/wt) ± SEMs (error bars) of triplicate experiments.

genes and comparing them with the ATCC 25586 sequences by a pairwise BLAST search (Table 2). The homologs in ATCC 23726 showed a high degree of similarity (97-100%) to ATCC 25586 homologs. The homologs identified in ATCC 25586 were considerably shorter than Fap2, with greatest similarity at the C-terminus, where the pore-forming transmembrane β-barrel is located in autotransporters. The C-terminus of each homolog showed similarity to the conserved autotransporter β-domain pfam03797.

Construction of the *aim*1 Mutant, *aim*less1

Using the gene sequence from *F. nucleatum* ATCC 25586 (Fn2058), we created primers to amplify a fragment of *aim*1. The amplified fragment was ligated into pHS31, creating integration plasmid pIP-*aim*1 (Fig. 1A). Transformation experiments yielded 16 thiamphenicol-resistant mutants (designated '*aim*less1'), whose growth was indistinguishable from that of the wild-type parent strain in normal culture conditions.

PCR analyses confirmed that pIP-*aim*1, as well as wild-type and the *aim*less1 genomic DNA, harbored the *aim*1 gene fragment (*aim*1′; Fig. 1B, panel 1). The *cat*P determinant was evident by PCR analyses in pIP-*aim*1 and in *aim*less1 genomic DNA, but, as predicted, was not present in the wild-type genome (Fig. 1B, panel 2). PCR analysis also confirmed the structure and site of vector integration, and ruled out the presence of a replicating plasmid carrying the *cat*P gene. Primers flanking *aim*1′ (*aim*1-5′F and *aim*1-3′R) amplified a 1.2-kb product from the wild-type chromosome, but, as expected, yielded no product from pIP-*aim*1 or *aim*less1 (Fig. 1B, panel 3). Flanking primers were used in combination with pHS31-specific primers (*cat*P-R and ColE1) to confirm the site of chromosomal integration. Expected 1.8-kb and 2.1-kb fragments were amplified for each primer pair (Fig. 1B, panels 6 and 7) from *aim*less1, but not from wild-type or pIP-*aim*1 DNA. This demonstrated specific integration of pIP-*aim*1 into the chromosome at the *aim*1 site, as predicted for a homologous recombination event.

Two genes downstream of *aim*1 could potentially be disrupted by plasmid integration (Fig. 1A). Real-time PCR transcriptional analyses of *aim*1 and downstream gene Fn2057 were conducted to confirm disruption of *aim*1 expression in *aim*less1, and to rule out the possibility of a polar effect on downstream genes. Two real-time PCR primer sets for the 3′ portion of *aim*1 showed that transcription levels of this region were at background levels in *aim*less1, 61-fold lower than in wild-type, indicating that the insertion disrupted transcription. Real-time PCR with primers for the 5′ portion of *aim*1 showed transcription levels similar to those of the wild type, indicating that this region was transcribed at normal levels. Importantly, primers for the downstream gene Fn2057 showed similar transcription levels in *aim*less1 and wild-type strains, indicating that expression of Fn2057 was not affected by vector integration (Fig. 1C).

Reduced Apoptosis-inducing Ability of the *aim*1 Mutant

We were interested in determining if *aim*1 contributed to the apoptosis phenotype. Incubation of Jurkat cells with *F. nucleatum* ATCC 23726 resulted in increased levels of apoptosis compared with that of Jurkat cells incubated alone. Our apoptosis assays showed that the number of apoptotic Jurkat cells present when incubated with wild-type *F. nucleatum* (14.2%) was significantly higher ($p < 0.0001$) than the number of apoptotic cells present when the cells were incubated with *aim*less1 mutant (11.2%), and both groups were significantly different from Jurkat cells incubated alone (6.9%). Thus, *aim*less1 demonstrated a 41.2% decrease in the number of apoptotic cells, indicating that *aim*1 plays a significant role in the induction of apoptosis (Fig. 2).

DISCUSSION

Evading host defense mechanisms is a critical element in bacterial pathogenesis. Previous studies have indicated that one aspect of *F. nucleatum* virulence is its induction of apoptosis in host lymphocytes (Jewett *et al.*, 2000). In this study, we identified homologs to the apoptosis-inducing protein Fap2 in the transformable *F. nucleatum* strain ATCC 23726, created an isogenic mutant for the *aim*1 gene, and demonstrated that the mutation impaired the ability of *F. nucleatum* to induce apoptosis. These findings document the first characterized mutation in *F. nucleatum*, and confirm the first apoptosis-inducing gene in this species. Together, these data provide a critical initial step in defining a genetic basis for *F. nucleatum* pathogenesis.

The creation of site-directed mutants represents a major advance in *F. nucleatum* research. Currently, genomic DNA sequences are available for 3 strains of *F. nucleatum*. The ATCC 23726 strain has not undergone genomic sequence analysis, but is related to the sequenced subspecies *nucleatum* strain ATCC 25586 at the subspecies level. Using the ATCC 25586 genomic sequence, we found that all 8 of the Fap2 homologs identified in the ATCC 25586 genome were present in ATCC 23726, and showed a high degree of similarity to the ATCC 25586 homologs over the sequenced fragment. Analysis of Fap2 showed that it contained 3 domains. The C-terminal autotransporter domain is predicted to be responsible for pore formation and transport of the protein to the cell surface. The central domain, occupying a majority of the protein, contains tandem and periodic repeats similar to those found in filamentous hemagglutinins and adhesins (Clantin *et al.*, 2004). The central and C-terminal domains of Fap2 are similar to those of Fap2 homologs identified in the ATCC 25586 genome, whereas the N-terminal domain remains distinct. The contribution of the N-terminal domain to inducing apoptosis is unknown, but truncation of this domain in the gene fragment recovered from the *E. coli* library indicates that it may have no role. The central domain sequences of the Fap2 homologs vary, but all contain tandem and periodic repeats, extending from their N-terminus to the C-terminal autotransporter domain. There is a high degree of similarity between the autotransporter domain of Fap2 and the homologs. Our findings clearly indicate that transcription of the 3′ region of *aim*1, encoding the autotransporter domain and the 3′ portion of the central domain, is blocked in *aim*less1. Thus, the truncated *aim*1 protein is probably not secreted. Additional investigation at a protein level should confirm these predictions.

Phenotypic analysis of *aim*less1 in comparison with the parental wild-type strain revealed a role for the *aim*1 protein in the induction of apoptosis of Jurkat cells. These findings validate the earlier results indicating that Fap2 confers the apoptosis-inducing phenotype in *E. coli*. Demonstration that the downstream gene Fn2057 is transcribed at wild-type levels in *aim*less1 rules out possible polar effects caused by the insertion (Fig. 1C). The ability to induce apoptosis in eukaryotic cells is not unique to *F. nucleatum*. Bacterial proteins that induce apoptosis have been identified in several pathogens, including the vacuolating toxin of *Helicobacter pylori* (Henderson and Nataro, 2001; Cover *et al.*, 2003), yet the molecular mechanisms by which these proteins cause disease have not been well-established. The *aim*1 mutation resulted in a partial, but highly reproducible, inhibition of Jurkat cell apoptosis. This

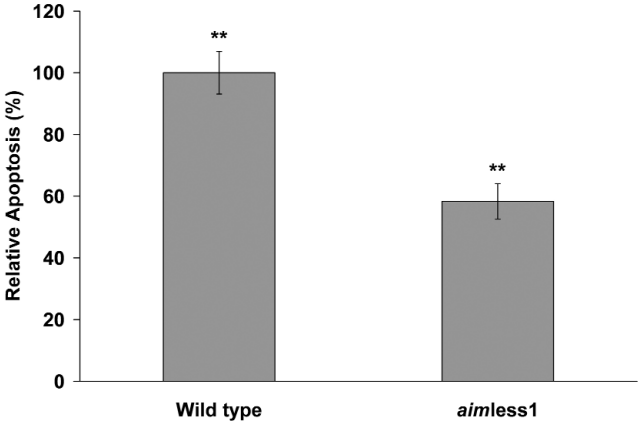

Figure 2. Induction of apoptosis in Jurkat cells after incubation with *F. nucleatum* wild-type or with *aim*less1. Jurkat cells were incubated with wild-type or *aim*less1 for 18 hrs before assay (n = 3). Uninfected Jurkat cells were incubated alone as a control. Values shown are relative to wild-type apoptosis levels after background subtraction. Error bars represent SD. **$p < 0.0001$.

is important, since it is likely that other *F. nucleatum* factors contribute to apoptosis induction, consistent with findings in other bacterial pathogens (Henderson and Nataro, 2001). The 7 additional Fap2 homologs are putative apoptosis-inducing OMPs, and studies are under way examining their potential role in pathogenesis. Two possible mechanisms of apoptosis induction by *F. nucleatum* OMPs have been hypothesized: (1) *F. nucleatum* OMPs directly deliver death signals through contact with lymphocyte cell-surface death receptors; and (2) *F. nucleatum*-mediated aggregation of lymphocytes allows lymphocyte death receptors to be crosslinked with their associated ligands on adjacent cells (Jewett *et al.*, 2000). The results presented in this study, demonstrating the role of *aim*1 in apoptosis, do not allow for a distinction between the two hypotheses. It is likely that multiple mechanisms lead to the induction of *F. nucleatum*-mediated apoptosis, indicating that further experiments are required to clarify the distinct mechanisms involved and how their synergistic effect contributes to apoptosis induction.

The generation of *aim*less1 was possible with the use of a new *F. nucleatum* integration vector. The site-specific chromosomal insertional mutagenesis demonstrated with pIP-*aim*1 is consistent with the accepted mechanism of homologous recombination. Additional vectors for molecular analysis in *F. nucleatum* include shuttle plasmids and an additional selectable marker conferring clindamycin resistance (Haake *et al.*, 2000), facilitating the mutagenesis of multiple genes, or mutagenesis and complementation of a single gene. Together, these tools allow for the molecular analysis of the *F. nucleatum* genome, and will aid in confirming the predicted function of genes with known homologs, as well as in determining the function of novel genes.

The induction of apoptosis in host lymphocytes provides a strategy that bacterial pathogens use to facilitate their survival through subverting the host innate immune response. The identification of *aim*1 as an *F. nucleatum* gene involved in suppressing the immune system represents an important first step in defining the molecular basis of *F. nucleatum* pathogenesis. The presence of additional Fap2 homologs in the

F. nucleatum genome indicates that further investigation of their function is warranted, and creation of additional gene inactivation mutants is under way.

ACKNOWLEDGMENTS

The authors acknowledge Julian I. Rood for providing the pJIR750 plasmid. This work was supported by Delta Dental grant WDS78956 (to W.S.) and by NIH/NIDCR PHS Grants No. DE12639 and DE015348 (to S.K.H.).

REFERENCES

Bolstad AI, Jensen HB, Bakken V (1996). Taxonomy, biology, and periodontal aspects of *Fusobacterium nucleatum*. *Clin Microbiol Rev* 9:55-71.

Clantin B, Hodak H, Willery E, Locht C, Jacob-Dubuisson F, Villeret V (2004). The crystal structure of filamentous hemagglutinin secretion domain and its implications for the two-partner secretion pathway. *Proc Natl Acad Sci USA* 101:6194-6199.

Cover TL, Krishna US, Israel DA, Peek RM Jr (2003). Induction of gastric epithelial cell apoptosis by *Helicobacter pylori* vacuolating cytotoxin. *Cancer Res* 63:951-957.

Edson RS, Rosenblatt JE, Washington JA 2nd, Stewart JB (1982). Gas-liquid chromatography of positive blood cultures for rapid presumptive diagnosis of anaerobic bacteremia. *J Clin Microbiol* 15:1059-1061.

Gonzalez-Gay MA, Sanchez-Andrade A, Cereijo MJ, Pulpeiro JR, Armesto V (1993). Pyomyositis and septic arthritis from *Fusobacterium nucleatum* in a nonimmunocompromised adult. *J Rheumatol* 20:518-520.

Haake SK, Yoder SC, Attarian G, Podkaminer K (2000). Native plasmids of *Fusobacterium nucleatum*: characterization and use in development of genetic systems. *J Bacteriol* 182:1176-1180.

Heckmann JG, Lang CJ, Hartl H, Tomandl B (2003). Multiple brain abscesses caused by *Fusobacterium nucleatum* treated conservatively. *Can J Neurol Sci* 30:266-268.

Henderson IR, Nataro JP (2001). Virulence functions of autotransporter proteins. *Infect Immun* 69:1231-1243.

Jewett A, Hume WR, Le H, Huynh TN, Han YW, Cheng G, *et al.* (2000). Induction of apoptotic cell death in peripheral blood mononuclear and polymorphonuclear cells by an oral bacterium, *Fusobacterium nucleatum*. *Infect Immun* 68:1893-1898.

Jousimies-Somer H, Savolainen S, Makitie A, Ylikoski J (1993). Bacteriologic findings in peritonsillar abscesses in young adults. *Clin Infect Dis* 16(Suppl 4):S292-S298.

Kapatral V, Anderson I, Ivanova N, Reznik G, Los T, Lykidis A, *et al.* (2002). Genome sequence and analysis of the oral bacterium *Fusobacterium nucleatum* strain ATCC 25586. *J Bacteriol* 184:2005-2018.

Kapatral V, Ivanova N, Anderson I, Reznik G, Bhattacharyya A, Gardner WL, *et al.* (2003). Genome analysis of *F. nucleatum sub spp vincentii* and its comparison with the genome of *F. nucleatum* ATCC 25586. *Genome Res* 13:1180-1189.

Merritt J, Qi F, Shi W (2005). A unique nine-gene comY operon in *Streptococcus mutans*. *Microbiology* 151:157-166.

Moore WE, Holdeman LV, Smibert RM, Good IJ, Burmeister JA, Palcanis KG, *et al*. (1982a). Bacteriology of experimental gingivitis in young adult humans. *Infect Immun* 38:651-667.

Moore WE, Holdeman LV, Smibert RM, Hash DE, Burmeister JA, Ranney RR (1982b). Bacteriology of severe periodontitis in young adult humans. *Infect Immun* 38:1137-1148.

Moore WE, Holdeman LV, Smibert RM, Cato EP, Burmeister JA, Palcanis KG, *et al.* (1984). Bacteriology of experimental gingivitis in children. *Infect Immun* 46:1-6.

Moore WE, Holdeman LV, Cato EP, Smibert RM, Burmeister JA, Palcanis KG, *et al.* (1985). Comparative bacteriology of juvenile periodontitis. *Infect Immun* 48:507-519.

Ribot S, Gal K, Goldblat MV, Eslami HH (1981). The role of anaerobic bacteria in the pathogenesis of urinary tract infections. *J Urol* 126:852-853.

Sabiston CB Jr, Gold WA (1974). Anaerobic bacteria in oral infections. *Oral Surg Oral Med Oral Pathol* 38:187-192.

Sundqvist GK, Eckerbom MI, Larsson AP, Sjögren UT (1979). Capacity of anaerobic bacteria from necrotic dental pulps to induce purulent infections. *Infect Immun* 25:685-693.

Talan DA, Citron DM, Abrahamian FM, Moran GJ, Goldstein EJC, The Emergency Medicine Animal Bite Infection Study Group (1999). Bacteriologic analysis of infected dog and cat bites. *N Engl J Med* 340:85-92.

Tatusova TA, Madden TL (1999). BLAST 2 sequences, a new tool for comparing protein and nucleotide sequences. *FEMS Microbiol Lett* 174:247-250.

Truant AL, Menge S, Milliorn K, Lairscey R, Kelly MT (1983). *Fusobacterium nucleatum* pericarditis. *J Clin Microbiol* 17:349-351.